


Article

Comparison of Pin Mill and Hammer Mill in the Fine Grinding of Sphagnum Moss

Ari Ämmälä 

Fiber and Particle Engineering Research Unit, Oulu University, 90014 Oulu, Finland; ari.ammala@oulu.fi

Abstract: Dried sphagnum moss was ground using a pin mill and a hammer mill under various operating conditions, i.e., changes in the rotor frequency and feed rate. The specific energy consumption of the size reduction was recorded. The ground powder was characterized by median particle size, width of size distribution (span), loose and tapped bulk densities, and the Hausner ratio. Pin milling used less energy for size reduction than hammer milling, especially when the target size was below 100 μm . In both milling methods, the specific energy consumption was mainly caused by the rotor frequency used. However, in pin milling, the specific energy consumption was also dependent on the production rate: the higher the rate, the higher the energy consumption. No such dependence was observed with the hammer mill. The span was wider in pin milling than hammer milling in the intermediate product size range although the difference decreased at the fine and coarse ends. A similar pattern was found for bulk densities. However, the flowability of powder, as characterized by the Hausner ratio, was comparable between the grinding methods.

Keywords: biomaterial; lignocellulose; peat; size reduction; pulverization; comminution; energy efficiency



Citation: Ämmälä, A. Comparison of Pin Mill and Hammer Mill in the Fine Grinding of Sphagnum Moss. *Energies* **2023**, *16*, 2437. <https://doi.org/10.3390/en16052437>

Academic Editors: Timo Kikas, Abrar Inayat and Lisandra Rocha Meneses

Received: 19 January 2023
Revised: 23 February 2023
Accepted: 28 February 2023
Published: 3 March 2023



Copyright: © 2023 by the author. Licensee MDPI, Basel, Switzerland. This article is an open access article distributed under the terms and conditions of the Creative Commons Attribution (CC BY) license (<https://creativecommons.org/licenses/by/4.0/>).

1. Introduction

In practice, the reduction in the size of biomass is always a prerequisite in any application. In the design and operation of particle and powder handling and processing equipment, there are three key properties to take into account when producing biomass powder: particle size distribution, energy consumption, and the flowability of powder.

The particle target size is primarily defined by the requirements for powder in the end application. A fine size is often advantageous because a large, available, specific surface area enhances thermo-chemical conversion, e.g., in combustion and pyrolysis [1–3]. However, lignocellulosic biomass tends to be recalcitrant in nature and the energy needed in fine grinding increases exponentially with decreasing particle size [4,5]. Thus, grinding biomass to a size that would be optimal in processing may be economically nonviable and will lead to a compromise between size reduction and energy consumption. Energy consumption depends on the characteristics of the raw material, its moisture content, grinding method, and target particle size [4,6], which is characterized by the mean, median, or mode of the size distribution, for example.

Flowability is important in the handling and storage of biomass powder and is dependent on interparticle cohesive and frictional forces. These are affected by the particle size distribution and shape [7], the physical and chemical surface properties of the particles, and the particles' density [8]. The Hausner ratio, calculated by dividing the compacted bulk density by the loose bulk density, is a commonly used index to give insight into the flow characteristics of powders [9]. It has been suggested that free-flowing, fairly free-flowing, and cohesive powders have Hausner ratios of 1.0–1.25, 1.25–1.4, and >1.4, respectively [10]. Cohesive powders have large surface attractions between particles due to the van der Waals force and electrostatic forces which overcome gravity; under these forces, particles can support themselves around voids in a powder bed [8]. A large volume of voids within

a poured bed produces a low, loose bulk density. The compaction of the bed by tapping generates forces that overcome the frictional forces and the cohesive attraction between particles, causing them to be rearranged and fall into void spaces, thus reducing the powder volume and consequently increasing its bulk density. The structure of a cohesive powder will consolidate significantly during tapping, whereas a free-flowing powder cannot be compacted significantly. Ground lignocellulose particles tend to be non-spherical, having a high aspect ratio (i.e., length-to-width ratio), which makes the flowability of biomass powder challenging [11].

A hammer mill is usually the first choice for size reduction [12]. In hammer mills, the breakage of particles is mainly due to the impacts of the rotating grinding elements, i.e., hammers, while the collision of particles onto the screen plate has a secondary effect [13]. The impact stress is proportional to the squared rotor tip speed, whereas the impact frequency is directly proportional to the rotor frequency [14]. The cumulative size-reduction effect is controlled by the time that particles stay within the grinding zone, which is strongly dependent on the screen design and the air flow through the screen openings caused by the rotor or auxiliary blower. Since size reduction is controlled by the screen, the size of the screen openings is the capacity-limiting factor in fine grinding. When small openings are used, there is also a risk of the screen plugging. Pin milling is a more robust method in this respect because screens are not used. Pin milling has been reported to grind materials to a finer particle size than hammer mills [15], but the lack of a screen may enlarge the width of size distribution [16]. The principal size-reduction mechanism is claimed to be impact in hammer milling and shear in pin milling [15]. In pin milling, however, the mechanism may depend on the dimensioning of the pin discs, i.e., the clearance between the pins, and on the size of the feed material. In pin mills, the grinding zone consists of a rotor and a stator disc (or two opposite rotating rotors) in which several rows of concentric circumferential pins alternate. The material travels between these pin rows towards the periphery due to centrifugal force and the air flow generated by the rotor. Particles larger than the pin clearance are torn by shear forces in the entrance of the grinding zone, after which size reduction takes place through impact forces. In fine grinding, impact is expected to be the main mechanism in both milling methods.

There are only a few published studies that compare the hammer mill and pin mill in the fine grinding of lignocelluloses or other biomaterials and that consider how operating parameters affect energy consumption and powder properties. For instance, results published for spices and seeds [17–19] are brief and inconclusive; in some cases, hammer milling has been more energy efficient, and in others, pin milling has been more energy efficient; in some instances, no significant difference has been found between the methods. It appears that grindability is dependent on material properties. Because lignocellulosic materials have an anisotropic physical and chemical structure on both macroscopic and microscopic scales, grindability cannot be evaluated from material properties but needs to be determined experimentally. The aim of this study was to investigate the interrelationship between size reduction, operating and design parameters, energy consumption, and the properties of powder produced in the fine grinding of a lignocellulose biomass with a pin mill and a hammer mill. Further, the aim was to find out which method is more energy efficient. The sphagnum moss used in the experiments is an abundant and productive plant, with an annual growth from 2.5 t/ha [20] up to 6.9 t/ha [21]. It grows in natural bogs but can also be farmed in a sustainable way [22], e.g., in cut-away peatlands. Sphagnum moss can be categorized as a lignocellulose material because its structural molecules are similar to those found in rooted plants [23].

2. Materials and Methods

The sphagnum moss was provided by Neova, Jyväskylä, Finland. The chemical composition of the sample was as follows: 4.3% extractives, 19.6% cellulose, 55.0% hemicelluloses, 21% Klason lignin, and 1.3% ash [13]. Before the fine grinding experiments, the moss sample was first dried at 60 °C, and then a batch of about 20 kg was pre-ground

and homogenized with a Rapid 40 knife mill equipped with a screen plate with 4 mm perforations. After knife milling, the median particle size was about 1.1 mm. The material density was 1510 kg/m³, measured with a helium pycnometer (Micrometrics, Norcross, GA, USA).

Fine grinding was performed with an Alpine Ultraplex 100 (Hosokawa-Alpine, Augsburg, Germany) in hammer milling mode using an impact rotor (Figure 1 top right), and in pin milling mode using a pinned rotor (Figure 1 top left) and stator. In hammer milling, three different screens were used: a smooth-contoured screen (Figure 1 bottom right) with 0.5 mm circular perforations (denoted as Ø0.5 mm), and rasp screens with trapezoidal openings inclined toward the rotation, with nominal sizes of 0.5 mm (Figure 1 bottom left) and 0.2 mm, respectively (denoted as #0.5 mm and #0.2 mm, respectively). The batch of size in grinding was 500 g in most cases but varied between 200 g and 700 g. The moisture content was 2–4%.

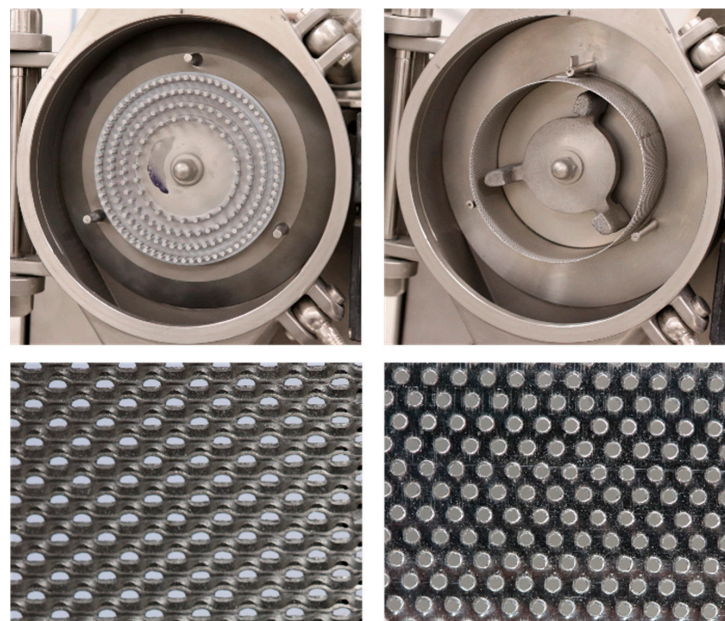


Figure 1. Pin mill rotor (top left) and hammer mill rotor (top right) used in experiments. Screen designs: rasp (bottom left) and smooth-contoured (bottom right).

Three rotor frequencies were used: 64, 185, and 303 s⁻¹ in hammer milling and 64, 202, and 370 s⁻¹ in pin milling. Tests were performed at two–three different production rates, controlled by the feed screw rotation frequency. Energy consumption was measured during grinding and without load. A weighed batch of sphagnum moss was ground, and the grinding time was recorded in order to calculate the production rate and specific energy consumption. Each grinding test was performed once without repetitions.

The net specific energy consumption (*SEC*, kWh/t) of the mill was calculated by subtracting the no-load power of the grinding system from the load power and dividing it by the production rate:

$$SEC = \frac{P - P_0}{m/t} \quad (1)$$

where *P* is the average power consumption of the grinding system during the grinding period, measured in W; *P*₀ is the power consumption of the grinding system in no-load conditions, measured in W; *m* is the oven dry mass of the ground powder batch, measured in kg; and *t* is the grinding time, measured in h.

The particle size distribution of the ground samples was measured using a method based on laser diffraction (Beckman Coulter LS 13320, Miami, FL, USA). Because of the high reproducibility of the method (in our internal monitoring, a coefficient of variation of 0.4% has been found for the median size), only one measurement per sample was performed.

The width of the distribution (*span*) was calculated based on [24] using the 90th, 10th, and 50th percentiles, as follows:

$$\text{span} = \frac{d_{90} - d_{10}}{d_{50}} \quad (2)$$

Bulk densities were measured according to SFS-EN 1236 (loose) and 1237 (tapped). Two parallel measurements were conducted for both loose and tapped bulk density. Based on the measurement data, the coefficient of variation was 0.8% for the former and 1.3% for the latter. The Hausner ratio was calculated by dividing the tapped bulk density, ρ_{tapped} , by the loose bulk density, ρ_{loose} :

$$\text{HR} = \frac{\rho_{\text{tapped}}}{\rho_{\text{loose}}} \quad (3)$$

FESEM (Zeiss Ultra Plus, Oberkochen, Germany) was employed to illustrate the particle morphology of the ground samples. Moisture-free samples were coated with carbon using an SEM sputter coater to improve the electric conductivity of the samples. The accelerating voltage during imaging was 5 kV.

3. Results and Discussion

3.1. Visual Appearance of Powder

Scanning electron microscope images of the ground moss in three degrees of fineness are shown in Figures 2–4. The particles tend to have an irregular, non-fibrous, yet elongated shape. In the case of coarse powders, the structural features of the plant are still apparent. Morphological uniformity increases when increased grinding energy is applied.

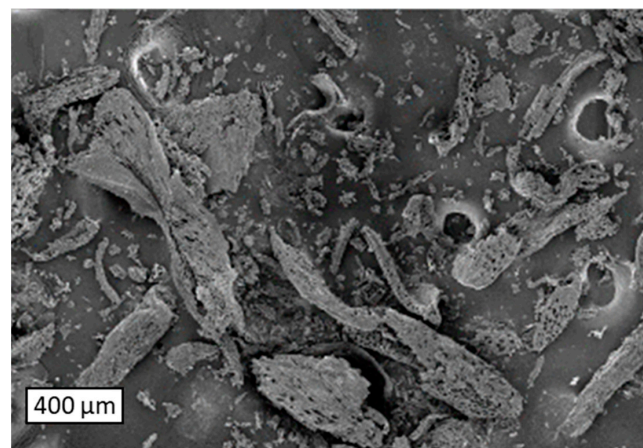


Figure 2. Powder ground with #0.5 rasp screen to a median size of 300 μm . Magnitude 150 \times .

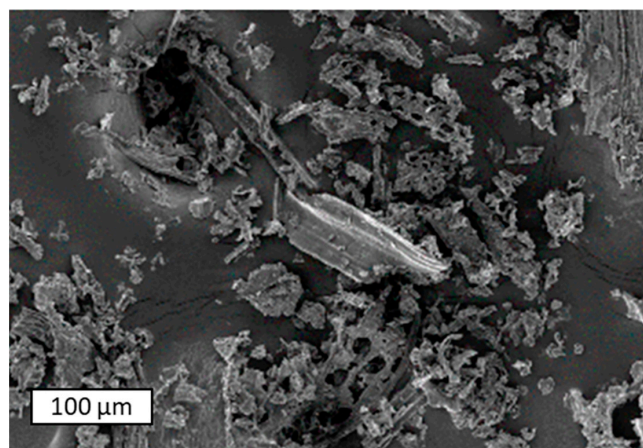


Figure 3. Powder ground with Ø0.5 smooth screen to a median size of 130 μm . Magnitude 500 \times .

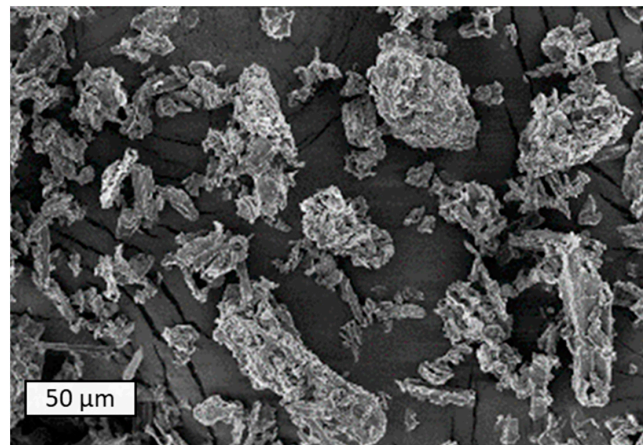


Figure 4. Powder ground with #0.2 rasp screen to a median size of 30 μm . Magnitude 1000 \times .

3.2. Particle Size Dependence on Production Rate and Rotor Frequency

In pin milling, an increasing production rate increased the particle size. Due to higher mass flow, the energy required for size reduction per mass unit decreased. However, the effect is quite low and, as shown in Figure 5, increasing the impact energy by increasing the rotor frequency has a decisive role in size reduction. The operating range was wide. The product size could vary in the range of 40–400 μm , primarily by adjusting the rotor frequency.

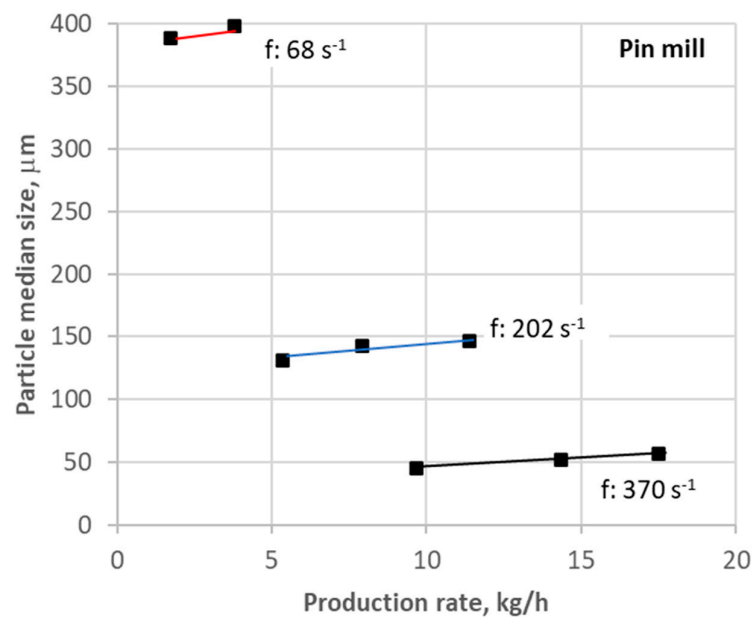


Figure 5. Dependence of particle size on production rate at three levels of rotor frequency ($f: 68 \text{ s}^{-1}$, 202 s^{-1} , and 370 s^{-1}) in pin milling.

In hammer milling, when screens were used to control the particle size in the product, the role of the production rate was more pronounced with the rasp screens than with the smooth screen (Figure 6). In the case of the rasp screens, particle size increased with an increasing production rate with the exception of the lowest rotor frequency. With the smooth screen, production rate had a minimal impact on particle size.

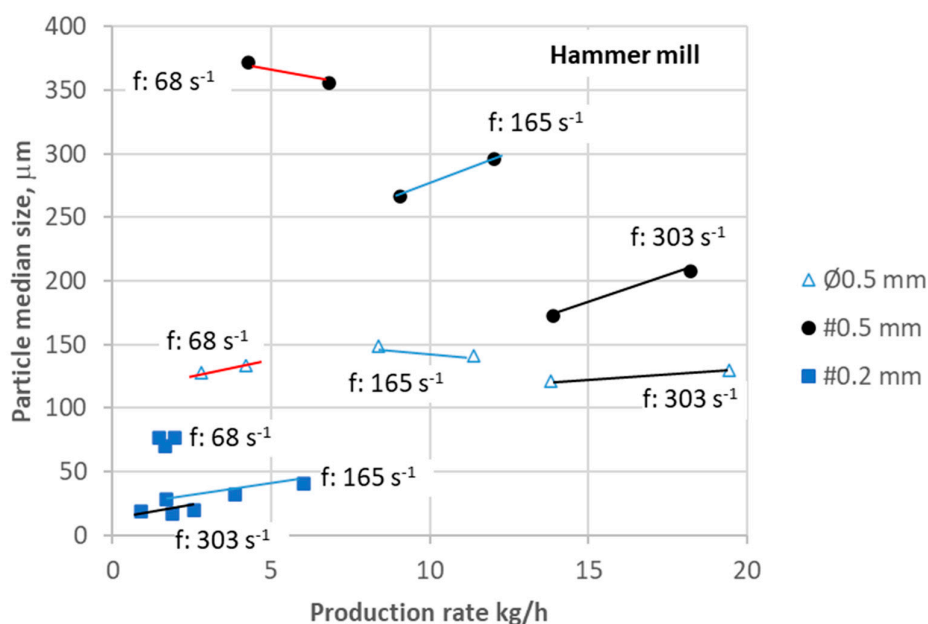


Figure 6. Dependence of particle size on the production rate at three levels of rotor frequency (f : 68 s^{-1} , 165 s^{-1} , and 303 s^{-1}) in hammer milling with different screen designs ($\text{Ø}0.5\text{ mm}$, $\#0.5\text{ mm}$, and $\#0.2\text{ mm}$).

The effect of rotor frequency was seen to be highly dependent on the screen design; with the smooth screen ($\text{Ø}0.5\text{ mm}$), the particle size of the product was almost independent of it, whereas with the rasp screen ($\#0.5\text{ mm}$), a linear relationship between the increasing rotor frequency and the decreasing particle size of the product was found. The difference could be explained with the help of the incident angle; this is because, in the rasp screens, the openings are inclined toward the trajectory of the particles, as governed by the tangential speed of the rotor and the radial drag force of the air flow generated by the rotor. However, flow patterns on the screen surface and within the screen openings may have a greater effect. The eddy formed within the openings reduces their effective open area [13], especially in the case of the smooth-surface screen, which may explain the smaller product particle size with the smooth screen in comparison with the rasp screen, when both have the same nominal size. This could also explain the general observation [12,25,26] that the particle size is many times smaller than the size of the openings.

With the $\#0.2\text{ mm}$ rasp screen, the production rate seemed to be sensitive to the rotor frequency. This may indicate that a powder bed existed on the screen that governed the passage of particles through the openings. When a low frequency (68 s^{-1}) was used, the particles did not disintegrate fast enough and the material started to accumulate within the mill; air flow rate generated by the rotor was low, which also contributed to this effect. At a high frequency (303 s^{-1}), although advantageous for the particle disintegration rate, the air flow rate generated was probably too high (proportional to the rotor frequency), which tended to force particles through the screen, causing them to crowd into the openings. At a frequency of 165 s^{-1} , the grinding run was stable and higher production rates could be used.

3.3. Particle Size vs. Energy Consumption

Based on the findings about the effect of particle size, production rate, rotor frequency, and screen design, it was expected that differences in specific energy consumption would be found as well. In general, the SEC and size reduction were strongly related to the rotor frequency used.

Besides rotor frequency, the SEC needed for size reduction in pin milling was clearly dependent on the production rate. Meanwhile, in hammer milling using rasp screens, the

production rate did not seem to affect the *SEC* directly; it was related to the particle size of the product (Figure 7). An apparent change in energy requirement appeared in pin milling at around 130–150 μm (seen clearly at the lowest production rate), which may indicate a change in the prevailing grinding mechanism from shear to impact. At particle sizes above 100 μm , size reduction with pin milling needed less grinding energy than hammer milling with the 0.5 mm screens when a low production rate was used. At higher production rates, however, the differences were reduced. Although the operation range is different for the smooth screen ($\text{\O}0.5$ mm) and the rasp screen ($\#0.5$ mm), extrapolation of the results indicates that about 40% less energy is needed for a particle size of around 150–200 μm with the rasp screen. With the smooth screen at the lowest rotor frequency, energy consumption was found to double (size of 133 μm and *SEC* of 24 kWh/t). This indicates that a low size-reduction rate together with an inadequate purging air flow rate caused the powder to accumulate inside the mill, and thus grinding was outside of its ideal operation range.

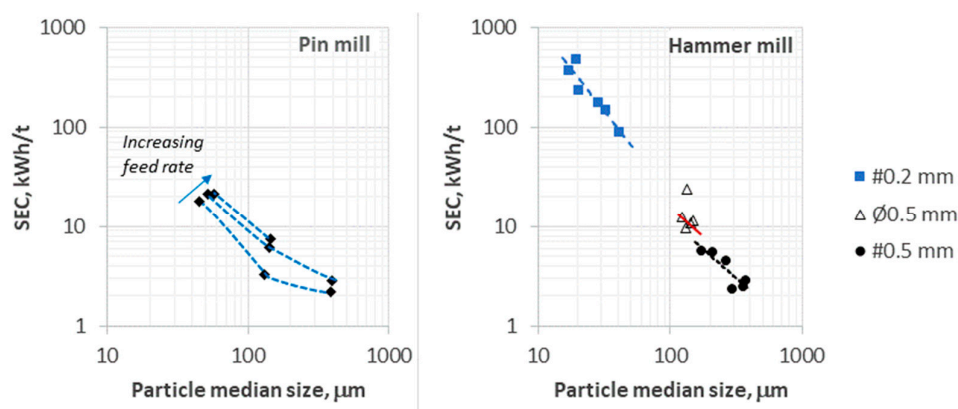


Figure 7. *SEC* as a function of particle size; pin mill in left, hammer mill in right. The dashed lines in pin milling emphasize the effect of the production rate.

In contrast, at particle sizes below 100 μm , size reduction with pin milling clearly needed less disintegration energy than hammer milling with the $\#0.2$ mm rasp screen (Figure 7). The smallest achievable particle size in one-pass, 45–57 μm (depending on production rate), required an *SEC* of 18–22 kWh/t. By extrapolation for the same size range, 60–70 kWh/t would be needed in hammer milling with the rasp screen of $\#0.2$ mm.

Sphagnum moss has much higher grindability than more common lignocelluloses, such as wood and straw, and the energy needed in fine grinding is an order of magnitude lower for a fine-sized powder [1].

3.4. Width of Size Distribution (Span)

The dependence of the span on the median particle size is illustrated in Figure 8. In the case of hammer milling with screens with a nominal size of 0.5 mm, the span remained almost unchanged (at about 2.3) within the size range of 100–400 μm , thus being independent of the screen design (smooth vs. rasp) or operating parameters used. When the sample was ground to below 100 μm using a screen of $\#0.2$ mm, the span widened monotonically from 2.3 to 5.3 with a decreasing median size from 100 to 20 μm , although the span began to narrow below 20 μm . The pin mill produced a slightly higher span than the hammer mill and the span increased linearly from 2.5 to 3.4, with a decreasing median size from 400 to 45 μm , respectively. However, at a size of around 40–50 μm , the span was equal in both grinding methods.

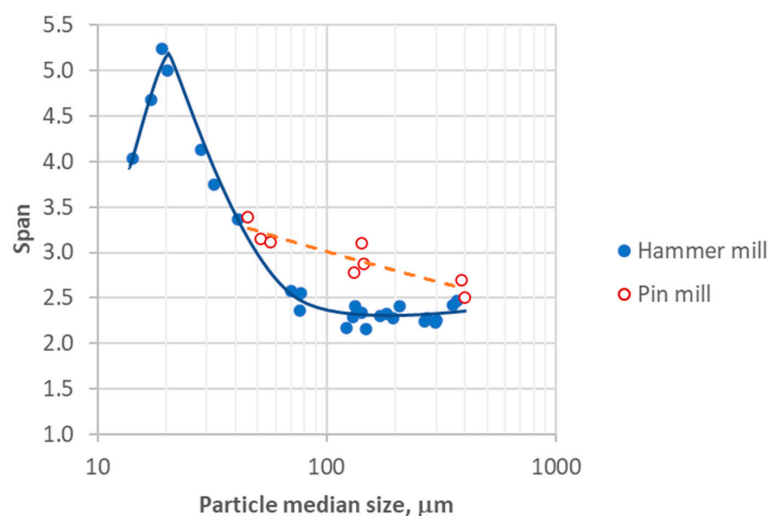


Figure 8. Span as a function of median particle size.

3.5. Bulk Density

Bulk densities were relatively low especially for the coarser powders, at 130–170 kg/m³ for loose packing within the particle size range of 200–400 μm . High friction and mechanical interlocking between particles having flaky irregular shapes result in a low loose bulk density [27]. During tapping, particles were able to be rearranged, producing a significantly consolidated powder column.

Both the loose and tapped bulk densities, shown in Figure 9, increased with a decreasing particle size, which is in line with the findings about the grinding of corn stover [12]. The increase was exponential in hammer milling, whereas in pin milling, the increase was close to linear. The screen design did not seem to affect the bulk density patterns of ground powder in hammer milling. The pin mill produced higher bulk densities than the hammer mill within the intermediate size range but there was no difference either at the large end (around 400 μm) or at the small end (around 40–50 μm). The width of the particle size distribution could be an explanation for this, since a similar pattern was seen in bulk densities and spans. As can be seen in Figure 7, the span was greater for the pin mill within the intermediate range. At the same particle size, a wider size distribution produces a higher bulk density [24], as can also be deduced from the results of Tannous et al. [28], where a wood powder sample combined from sieved fractions (wide span) had a higher bulk density than a fraction of the same size (narrow span).

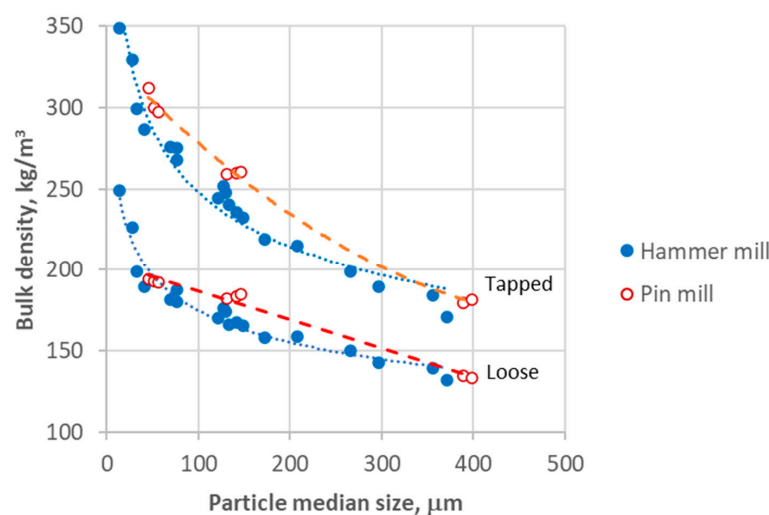


Figure 9. Loose and tapped bulk densities as a function of particle size.

Increasing bulk densities have been reported for many biomaterials. One explanation could be that particle density increases with a decreasing particle size due to less porous particles [26]. Additionally, the shape of particles is expected to alter from irregular, flake-like particles to more spherical particles, which is known to increase bulk density [26]. However, increasing cohesiveness with decreasing size often has a detrimental effect on loose bulk density. With wood powder, for instance, it was found to be fairly constant from 150 to 35 μm , whereas tapped bulk density clearly increased [5]. Thus, the synergistic effects of particle size and shape (and their distributions), together with the chemical state of the particle surfaces, resulted in less cohesion of fine sphagnum moss powder. More detail is given about this in the following section.

3.6. Hausner Ratio

The Hausner ratio is an often-used parameter to give an idea of the flowability of powders, and it is linearly correlated to the cohesiveness of the powder [29]. There is a reasonable correlation between the Hausner ratio and the angle of repose [9], and flow characteristics can be classified into seven categories [8], as illustrated in Figure 10. The Hausner ratio can also be applied to distinguish the free-flowing, easy-to-fluidize group A powders from the cohesive, hard-to-fluidize group C powders [30]. Cohesive powders have a ratio greater than 1.4, whereas powders in group A have a ratio of less than 1.25.

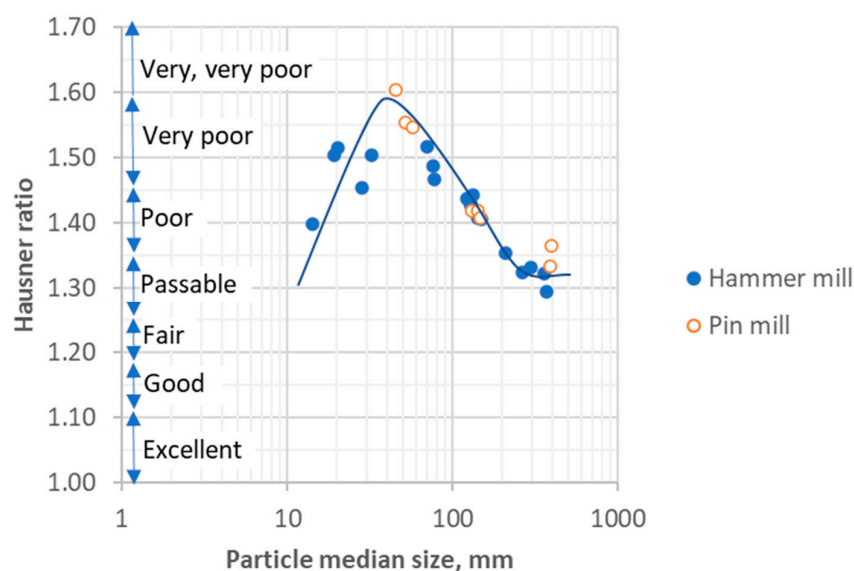


Figure 10. Hausner ratio as a function of median size. Flow characterization according to Fitzpatrick [3].

The milling method did not considerably affect the Hausner ratio, which seemed to depend mainly on particle size. Three distinct phases were seen (Figure 10). With coarse powder having a median size greater than 200 μm , the Hausner ratio was fairly constant at 1.33, indicating passable flow properties. This is in accordance with findings for wood powder [28]. When the size decreased from 200 to 40 μm , the Hausner ratio increased from 1.33 to 1.6 (from passable to very, very poor flowability). This is less than that reported for wood powder with a similar size range [5], where the ratio increased from 1.4 to over 2. The increasing Hausner ratio is interpreted as increased cohesiveness due to increased surface area and van de Waals attraction. However, when the size decreased further, to below about 40 μm , the Hausner ratio decreased sharply from 1.6 to 1.4, signifying reduced interaction between particles. This could be related to the changes in the chemical composition of the surfaces, since a lignocellulosic structure is not chemically isotropic and the surfaces exposed in ultrafine grinding are chemically changed, affecting the interaction between ultrafine particles [31]. Finely ground sphagnum moss has been

measured to be hydrophobic, having a contact angle order of 105° with water [32], and hydrophobic surfaces have been found to be beneficial to the flowability of fine-sized powders [33]. It may also be possible that the generation of submicron particles starts to act as a flow additive, enhancing flowing properties and increasing bulk densities [34]. Chemical heterogeneity between particles is expected to increase as well, and lignin-rich, hemicellulose-rich, and cellulose-rich particles can be found that may be a reason for decreasing cohesiveness. The morphological uniformity of particles probably increases, as also seen in the decreasing span shown in Figure 8, which may play its own synergetic role in the Hausner ratio.

Although improved flowability of very fine powder may seem implausible, a similar pattern has been found in the fine grinding of the same material with an air classifier mill [35]. Moreover, it has been reported that the micronization of biomaterials can indeed increase their flowability [36]. For example, for wheat bran powder having a median size of $102\ \mu\text{m}$ and a Hausner ratio of 1.73, micronization with a vibration mill was found to decrease the Hausner ratio linearly from 1.82 to 1.15, whereas the median size decreased from 32 to $22\ \mu\text{m}$ [37].

4. Conclusions

Sphagnum moss was found to be easy to grind in comparison to other materials, such as wood and straw. Pin milling appears to be a better method for the fine grinding of this kind of material than hammer milling. It is more energy efficient, especially if the target size is below $100\ \mu\text{m}$. Pin milling also has a higher capacity for a fine-sized powder product and is not prone to plugging as hammer milling is, which uses a screen with small openings. The width of size distribution is larger in pin milling, but the difference seems to disappear in fine-sized powders. Additionally, loose and tapped bulk densities tend to be higher in pin milling. However, the flowability of powders characterized by the Hausner ratio is equivalent for both grinding methods at any given particle size. Interestingly, flowability was found to decrease with decreasing particle size but only to a certain critical size, below which flowability improved [35].

Funding: Council of Oulu Region (grant A71069 aided by the European Regional Development Fund), Neova Oy (former Vapo), and Haarla Oy.

Data Availability Statement: Data are available from the author upon request.

Acknowledgments: I would like to thank Jarno Karvonen for his contribution to the fine grinding experiments and particle size measurements, and Elisa Wirkkala for her contribution to the bulk density measurements.

Conflicts of Interest: The author declares no conflict of interest.

References

1. Karinkanta, P.; Ämmälä, A.; Illikainen, M.; Niinimäki, J. Fine Grinding of Wood—Overview from Wood Breakage to Applications. *Biomass Bioenergy* **2018**, *113*, 31–44. [\[CrossRef\]](#)
2. Hansson, J.; Berndes, G.; Johnsson, F.; Kjärstad, J. Co-Firing Biomass with Coal for Electricity Generation—An Assessment of the Potential in EU27. *Energy Policy* **2009**, *37*, 1444–1455. [\[CrossRef\]](#)
3. Dai, J.; Saayman, J.; Grace, J.R.; Ellis, N. Gasification of Woody Biomass. *Annu. Rev. Chem. Biomol. Eng.* **2015**, *6*, 77–99. [\[CrossRef\]](#) [\[PubMed\]](#)
4. Temmerman, M.; Jensen, P.D.; Hébert, J. Von Rittinger Theory Adapted to Wood Chip and Pellet Milling, in a Laboratory Scale Hammermill. *Biomass Bioenergy* **2013**, *56*, 70–81. [\[CrossRef\]](#)
5. Wang, J.; Gao, J.; Brandt, K.L.; Wolcott, M.P. Energy Consumption of Two-Stage Fine Grinding of Douglas-Fir Wood. *J. Wood Sci.* **2018**, *64*, 338–346. [\[CrossRef\]](#)
6. Adapa, P.; Tabil, L.; Schoenau, G. Grinding Performance and Physical Properties of Non-Treated and Steam Exploded Barley, Canola, Oat and Wheat Straw. *Biomass Bioenergy* **2011**, *35*, 549–561. [\[CrossRef\]](#)
7. Pachón-Morales, J.; Colin, J.; Casalinho, J.; Perré, P.; Puel, F. Flowability Characterization of Torrefied Biomass Powders: Static and Dynamic Testing. *Biomass Bioenergy* **2020**, *138*, 105608. [\[CrossRef\]](#)
8. Fitzpatrick, J. Powder Properties in Food Production Systems. In *Handbook of Food Powders*; Elsevier: Amsterdam, The Netherlands, 2013; pp. 285–308; ISBN 978-0-85709-513-8.

9. Kalman, H. Quantification of Mechanisms Governing the Angle of Repose, Angle of Tilting, and Hausner Ratio to Estimate the Flowability of Particulate Materials. *Powder Technol.* **2021**, *382*, 573–593. [[CrossRef](#)]
10. Santomaso, A.; Lazzaro, P.; Canu, P. Powder Flowability and Density Ratios: The Impact of Granules Packing. *Chem. Eng. Sci.* **2003**, *58*, 2857–2874. [[CrossRef](#)]
11. Xu, G.; Li, M.; Lu, P. Experimental Investigation on Flow Properties of Different Biomass and Torrefied Biomass Powders. *Biomass Bioenergy* **2019**, *122*, 63–75. [[CrossRef](#)]
12. Tumuluru, J.; Heikkilä, D. Biomass Grinding Process Optimization Using Response Surface Methodology and a Hybrid Genetic Algorithm. *Bioengineering* **2019**, *6*, 12. [[CrossRef](#)] [[PubMed](#)]
13. Ämmälä, A.; Pääkkönen, T.M.; Illikainen, M. Role of Screen Plate Design in the Performance of a Rotor Impact Mill in Fine Grinding of Biomass. *Ind. Crops Prod.* **2018**, *122*, 384–391. [[CrossRef](#)]
14. Austin, L.G. A Preliminary Simulation Model for Fine Grinding in High Speed Hammer Mills. *Powder Technol.* **2004**, *143–144*, 240–252. [[CrossRef](#)]
15. Mayer-Laigle, C.; Rajaonarivony, R.; Blanc, N.; Rouau, X. Comminution of Dry Lignocellulosic Biomass: Part II. Technologies, Improvement of Milling Performances, and Security Issues. *Bioengineering* **2018**, *5*, 50. [[CrossRef](#)]
16. Lomovskiy, I.; Bychkov, A.; Lomovsky, O.; Skripkina, T. Mechanochemical and Size Reduction Machines for Biorefining. *Molecules* **2020**, *25*, 5345. [[CrossRef](#)]
17. Meghwal, M.; Goswami, T.K. Comparative Study on Ambient and Cryogenic Grinding of Fenugreek and Black Pepper Seeds Using Rotor, Ball, Hammer and Pin Mill. *Powder Technol.* **2014**, *267*, 245–255. [[CrossRef](#)]
18. Shashidhar, M.G.; Murthy, T.P.K.; Girish, K.G.; Manohar, B. Grinding of Coriander Seeds: Modeling of Particle Size Distribution and Energy Studies. *Part. Sci. Technol.* **2013**, *31*, 449–457. [[CrossRef](#)]
19. Tangirala, S.; Charithkumar, K.; Goswami, T.K. Modeling of Size Reduction, Particle Size Analysis and Flow Characterisation of Spice Powders Ground in Hammer and Pin Mills. *Int. J. Res. Eng. Technol.* **2014**, *3*, 296–309. [[CrossRef](#)]
20. Silvan, N. Sphagnum farming: A quick restoration for cut-away peatlands. In *Peatlands International*; International Peatland Society: Jyväskylä, Finland, 2010; pp. 24–25.
21. Gaudig, G.; Fengler, F.; Krebs, M.; Prager, A.; Schulz, J.; Wichmann, S.; Joosten, H. Sphagnum Farming in Germany—A Review of Progress. *Mires Peat* **2014**, *13*, 1–11.
22. Pouliot, R.; Hugron, S.; Rochefort, L. Sphagnum Farming: A Long-Term Study on Producing Peat Moss Biomass Sustainably. *Ecol. Eng.* **2015**, *74*, 135–147. [[CrossRef](#)]
23. Ämmälä, A.; Piltonen, P. Sphagnum Moss as a Functional Reinforcement Agent in Castor Oil-Based Biopolyurethane Composites. *Mires Peat* **2019**, *24*, 1–11. [[CrossRef](#)]
24. Deng, Y.; Dewil, R.; Appels, L.; Zhang, H.; Li, S.; Baeyens, J. The Need to Accurately Define and Measure the Properties of Particles. *Standards* **2021**, *1*, 19–38. [[CrossRef](#)]
25. Naimi, L.J.; Sokhansanj, S.; Bi, X.; Lim, C.J.; Womac, A.R.; Lau, A.K.; Melin, S. Development of Size Reduction Equations for Calculating Energy Input for Grinding Lignocellulosic Particles. *Appl. Eng. Agric.* **2013**, *29*, 93–100. [[CrossRef](#)]
26. Mani, S.; Tabil, L.G.; Sokhansanj, S. Grinding Performance and Physical Properties of Wheat and Barley Straws, Corn Stover and Switchgrass. *Biomass Bioenergy* **2004**, *27*, 339–352. [[CrossRef](#)]
27. Carson, L.; Pittenger, B. Bulk Properties of Powders. In *Powder Metal Technologies and Applications*; Eisen, W., Ferguson, B., German, R., Iacocca, R., Lee, P., Madan, D., Moyer, K., Sanderow, H., Trudel, Y., Eds.; ASM Handbook; ASM International: Russel Township, OH, USA, 1998; Volume 7, pp. 287–301.
28. Tannous, K.; Lam, P.S.; Sokhansanj, S.; Grace, J.R. Physical Properties for Flow Characterization of Ground Biomass from Douglas Fir Wood. *Part. Sci. Technol.* **2013**, *31*, 291–300. [[CrossRef](#)]
29. Saw, H.Y.; Davies, C.E.; Paterson, A.H.J.; Jones, J.R. Correlation between Powder Flow Properties Measured by Shear Testing and Hausner Ratio. *Procedia Eng.* **2015**, *102*, 218–225. [[CrossRef](#)]
30. Abdullah, E.C.; Geldart, D. The Use of Bulk Density Measurements as Flowability Indicators. *Powder Technol.* **1999**, *102*, 151–165. [[CrossRef](#)]
31. Yang, Y.; Ji, G.; Xiao, W.; Han, L. Changes to the Physicochemical Characteristics of Wheat Straw by Mechanical Ultrafine Grinding. *Cellulose* **2014**, *21*, 3257–3268. [[CrossRef](#)]
32. Koivuranta, E.; Hietala, M.; Ämmälä, A.; Oksman, K.; Illikainen, M. Improved Durability of Lignocellulose-Polypropylene Composites Manufactured Using Twin-Screw Extrusion. *Compos. Part A Appl. Sci. Manuf.* **2017**, *101*, 265–272. [[CrossRef](#)]
33. Todorova, Z.; Wünsche, S.; Hintz, W. Improved Flowability of Ultrafine, Cohesive Glass Particles by Surface Modification Using Hydrophobic Silanes. In *Particles in Contact*; Antonyuk, S., Ed.; Springer International Publishing: Cham, Switzerland, 2019; pp. 631–662; ISBN 978-3-030-15898-9.
34. Blümel, C.; Sachs, M.; Laumer, T.; Winzer, B.; Schmidt, J.; Schmidt, M.; Peukert, W.; Wirth, K.-E. Increasing Flowability and Bulk Density of PE-HD Powders by a Dry Particle Coating Process and Impact on LBM Processes. *Rapid Prototyp. J.* **2015**, *21*, 697–704. [[CrossRef](#)]
35. Ämmälä, A. *Fine Grinding of Sphagnum Moss with ZPS Rotor Impact Mill Integrated with ATP Air Classifier*; University of Oulu: Oulu, Finland, 2018; Unpublished data.

36. Gao, W.; Chen, F.; Wang, X.; Meng, Q. Recent Advances in Processing Food Powders by Using Superfine Grinding Techniques: A Review. *Compr. Rev. Food Sci. Food Saf.* **2020**, *19*, 2222–2255. [[CrossRef](#)] [[PubMed](#)]
37. He, S.; Li, J.; He, Q.; Jian, H.; Zhang, Y.; Wang, J.; Sun, H. Physicochemical and Antioxidant Properties of Hard White Winter Wheat (*Triticum Aestivum* L.) Bran Superfine Powder Produced by Eccentric Vibratory Milling. *Powder Technol.* **2018**, *325*, 126–133. [[CrossRef](#)]

Disclaimer/Publisher’s Note: The statements, opinions and data contained in all publications are solely those of the individual author(s) and contributor(s) and not of MDPI and/or the editor(s). MDPI and/or the editor(s) disclaim responsibility for any injury to people or property resulting from any ideas, methods, instructions or products referred to in the content.